JOURNAL OF PHYSICAL ORGANIC CHEMISTRY
J. Phys. Org. Chem. 2005; **18:** 719–724
Published online 19 April 2005 in Wiley InterScience (www.interscience.wiley.com). DOI: 10.1002/poc.923

Theoretical estimation of the annular tautomerism of indazoles†

Ibon Alkorta* and José Elguero

Instituto de Química Médica, CSIC, Juan de la Cierva 3, E-28006 Madrid, Spain

Received 22 December 2004; revised 31 January 2005; accepted 7 February 2005

ABSTRACT: Theoretical calculations at semi-empirical AM1 and density functional B3LYP/6–31G* levels were carried out on 52 N*H*-indazoles. Although in most cases the 1*H*-tautomer is the most stable, we found several indazoles for which the 2*H*-tautomer is more stable than the 1*H*-tautomer. The differences in energy between the 1*H*- and 2*H*-tautomers were interpreted in terms of substituent effects with the use of a Free–Wilson (presence–absence) matrix. Copyright © 2005 John Wiley & Sons, Ltd.

KEYWORDS: indazole; tautomerism; AM1; B3LYP; Free–Wilson models

INTRODUCTION

The annular tautomerism of indazole (**1**) has been thoroughly studied from both experimental and theoretical points of view. The present knowledge was summarized by Minkin *et al*. in 2000.[1] The main conclusions are that the 1*H*-tautomer **1a** is more stable than the 2*H*-tautomer **1b** by 15.1 kJ mol^{-1} (MP2/6–31G*), which is characterized also by $\Delta G^{\circ}_{298.15} = 17.2\,\text{kJ mol}^{-1}$ when thermal energy correction and entropy effects are taken into account.[2] Recently, using semi-empirical methods, including AM1, Ögretir and Kaypak showed that the tautomerism of indazole (**1**), 3-methylindazole (**2**), 3-chloroindazole and 3-bromoindazole was not affected by the substituent at position 3.[3]

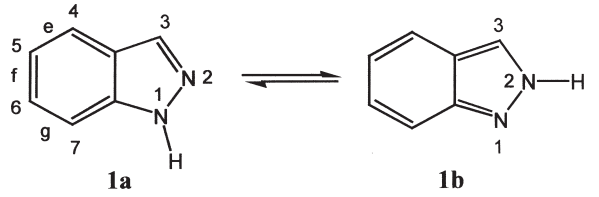

1a **1b**

Scheme 1 shows the structures of compounds **18a** and **35a**, selected for their biological significance. 1*H*-Pyrazolo[3,4-*d*]pyrimidine (**18a**) is the parent structure of a number of drugs, the best known being allopurinol,[4,5] but many other derivatives have also been reported. 1*H*-Pyrazolo[3,4-*b*]quinoline (**35a**) has shown different biological activities associated with the GABA receptors.[6]

**Correspondence to:* I. Alkorta, Instituto de Química Médica, CSIC, Juan de la Cierva 3, E-28006 Madrid, Spain.
E-mail: ibon@iqm.csic.es
Contract/grant sponsor: DGICYT; *contract/grant numbers:* SAF2003-08003-C02-02; BQU-2000-0906.
†Selected paper presented for a special issue dedicated to Professor Otto Exner on the occasion of his 80th birthday.

Concerning tautomerism, in addition to the information already reported about indazole (**1**), the data are mostly qualitative. For instance, for 3-substituted indazoles, 3-methylindazole exists as tautomer **2a** (gas phase),[7] 3-phenylindazole in the **3a** form (solution and solid state),[8] 3-methoxycarbonylindazole as the tautomer **5a** (solid state),[9] 3-methoxyindazole as **8a** (solution),[10] and 3-fluoroindazole as **9a** (solution).[11] Compound **18a** exists as represented (solid state and solution).[5] Concerning benzo-fused indazoles, benzo[*g*]indazole exists as **28a** (solution).[12]

The aims of the present paper are as follows: (i) to discuss the annular tautomerism of indazoles; (ii) to try additive models of the substituent effects on the calculated differences in energies; (iii) to search for relationships between inexpensive semi-empirical methods and mixed DFT–*ab initio* methods; and (iv) to try to find indazoles where the 2*H*-tautomer becomes predominant. Numerically calculated values containing no errors should not be analyzed statistically. However, it is sometimes useful to treat them as experimental values.

COMPUTATIONAL DETAILS

The AM1 calculations were carried using the Chem3D program.[13] The *ab initio* and DFT calculations were performed utilizing the Gaussian 98 package.[14] The geometries were optimized at the B3LYP/6–31G* computational level and were confirmed to be minimum structures by calculating the harmonic frequencies.[15–17] The entropic and enthalpic corrections to the energy were evaluated at the same computational level in order to obtain the free energies of the molecules. Additional calculations on the indazole molecule (**1**) were performed at the B3LYP/6–311 + G** and G2 levels.[18,19]

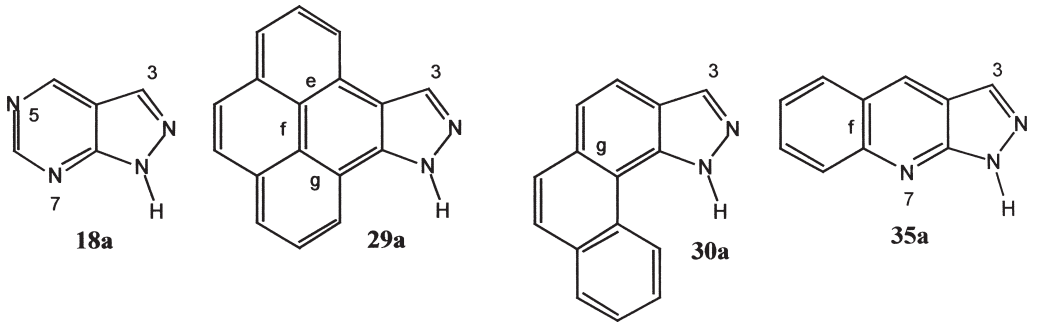

Scheme 1. Selected examples to illustrate structural modifications of the indazole ring studied here

RESULTS AND DISCUSSION

Set of compounds studied

We chose to study three structural modifications of the indazole ring:

1. The substituent at position 3 of the indazole ring: H, **1**; CH_3, **2**; C_6H_5, **3**; CN, **4**; CO_2CH_3, **5**; CF_3, **6**; NO_2, **7**; OCH_3, **8**; F, **9**.
2. The replacement of the benzene CH groups by N atoms: 4-aza, **10**; 5-aza, **11**; 6-aza, **12**; 7-aza, **13**; 4,5-diaza, **14**; 4,6-diaza, **15**; 4,7-diaza, **16**; 5,6-diaza, **17**; 5,7-diaza, **18**; 6,7-diaza, **19**; 4,5,6-triaza, **20**; 4,5,7-triaza, **21**; 4,6,7-triaza, **22**; 5,6,7-triaza, **23**; 4,5,6,7-tetraaza, **24**.
3. The fusion of a benzene ring to positions [*e*] (45), [*f*] (56) and [*g*] (67): [*e*], **25**; [*f*], **26**; [*g*], **27**; [*e*,*g*], **28**; [*efg*] (phenanthro), **29**; naphtho[*g*], **30**.

We then combined the second and third modifications: [*e*]-6-aza, **31**; [*e*]-7-aza, **32**; [*e*]-6,7-diaza, **33**; [*f*]-4-aza, **34**; [*f*]-7-aza, **35**; [*f*]-4,7-diaza, **36**; [*g*]-4-aza, **37**; [*g*]-5-aza, **38**; [*g*]-4,5-diaza, **39**. Illustrated (Scheme 1 where only the 1*H*-tautomer, **a** is represented) are some examples of these compounds.

AM1 calculations

These inexpensive and almost instantaneous calculations (for compounds of the size and geometry of those studied in this paper) are useful for exploring a large series of compounds. The results are reported in Table 1.

Since these values are all positive, tautomer 1*H***a** is always the most stable. For the parent indazole **1**, a value of 27.45 kJ mol^{-1} overestimates the best theoretical value of 17.2 kJ mol^{-1} by about 10 kJ mol^{-1}.

Using a Free–Wilson model (presence–absence matrix),[20] these 39 $\Delta\Delta E$ data can be interpreted in terms of individual contributions. A preliminary multi-regression (not shown) leads to the conclusion that the contributions of 3-CN and 3-CF_3 substituents are not significant. Therefore, they were omitted and the multi-regression repeated (Table 2, $n = 39$, $r^2 = 0.968$, F-value 46.5, P-value <0.0001).

We have reported the discussion of the individual substituent contributions to the DFT calculations section. The contributions of Table 2 allow to select some new

Table 1. Differences in energy $\Delta\Delta E$ (tautomer **b**—tautomer **a**) in kJ mol^{-1}

Compound	$\Delta\Delta E$
1	27.45
2	22.51
3	20.21
4	27.70
5	13.82
6	26.90
7	15.36
8	30.92
9	22.05
10	21.51
11	26.28
12	22.84
13	37.03
14	19.83
15	17.70
16	31.59
17	20.59
18	34.89
19	31.76
20	13.35
21	27.53
22	25.36
23	27.91
24	18.79
25	14.98
26	42.09
27	14.98
28	8.58
29	6.15
30	16.82
31	9.83
32	24.77
33	18.70
34	39.87
35	55.02
36	51.92
37	10.13
38	13.56
39	7.45

Table 2. Individual substituent contributions in kJ mol^{-1} (Free–Wilson model of $\Delta\Delta E$)[a]

Substituent	Value	Substituent	Value	Substituent	Value
3-Me	-4.3 ± 2.8	4-N	-4.4 ± 1.0	Benzo[*e*]	-9.6 ± 1.4
3-Ph	-6.6 ± 2.8	5-N	-3.3 ± 1.2	Benzo[*f*]	17.7 ± 1.6
3-CO_2CH_3	-13.0 ± 2.8	6-N	-5.1 ± 1.1	Benzo[*g*]	-10.9 ± 1.5
3-NO_2	-11.4 ± 2.8	7-N	9.8 ± 1.0	Phenanthro	-20.6 ± 2.8
3-OCH_3	4.1 ± 2.8			Naphtho[*g*]	-10.0 ± 2.8
3-F	-4.7 ± 2.8				

[a] Intercept 26.8 ± 1.0.

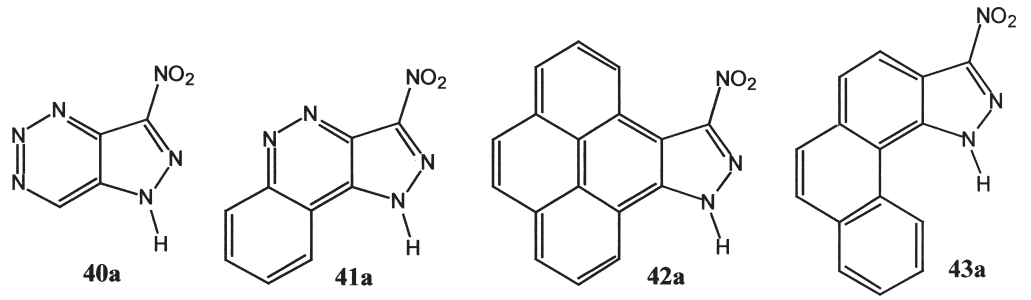

Scheme 2. 3-Nitroindazoles as candidates for increased stability of the 2*H*-tautomer **b**

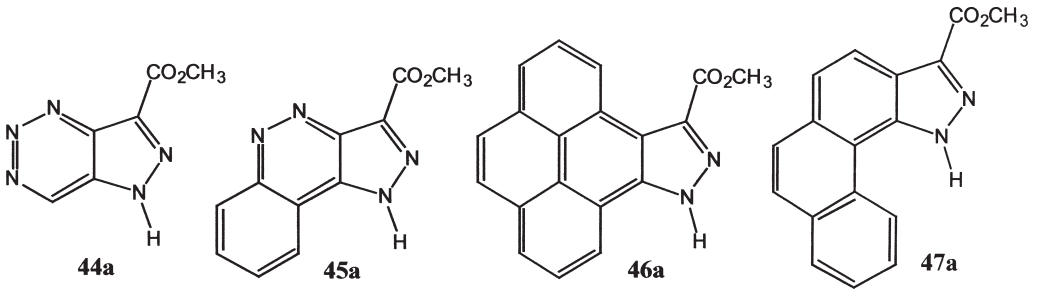

Scheme 3. Indazole-3-carboxylic acid methyl esters as candidates for increased stability of the 2*H*-tautomer **b**

molecules to have the lower values of $\Delta\Delta G$ and, if possible, negative values: (i) using the -11.4 kJ mol^{-1} effect of the 3-nitro group (Scheme 2) and (ii) using the -13.0 kJ mol^{-1} effect of the 3-ester group (Scheme 3).

We have summarized in Table 3 the predicted values using the estimated substituent contributions in Table 2 and also the AM1 directly calculated values (all values relative to parent indazole **1**, 27.45 kJ mol^{-1}).

Only in the case of **42** and, to a lesser extent, **46** (both phenanthro derivatives) does the additive model fail, but several possible candidates for our project have been found: **41**, **45** and **46**, all of them with negative $\Delta\Delta E$ values.

Table 3. Predicted (regression lines) and calculated (AM1) energy values for 3-NO_2 and 3-CO_3CH_3 indazoles in kJ mol^{-1}

Compound	$\Delta\Delta E$[a]	$\Delta\Delta E$ (AM1)	Difference
40	2.6 ± 3.1	2.45	-0.1
41	-3.2 ± 3.2	-1.56	1.6
42	-5.3 ± 3.8	0.02	5.3
43	5.4 ± 3.8	6.15	0.8
44	1.1 ± 3.1	0.14	-0.9
45	-4.7 ± 3.2	-4.73	0.0
46	-6.8 ± 3.8	-9.57	-2.7
47	3.8 ± 3.8	4.22	0.4

[a] Based on the regression line with parameters given in Table 2.

The Mills–Nixon effect as an auxiliary to shift the tautomerism of indazoles

We have used, and amply discussed in three papers, the bond localization of the Mills–Nixon effect, to modify the tautomerism of NH-pyrazoles.[21] The presence of a benzene ring between the small saturated ring and the pyrazole ring should weaken the bond localization effects (Scheme 4).

According to the AM1 calculations, in all three cases the 1*H*-tautomer predominates (**48**, 35.77; **49**, 16.57; **50**, 37.70 kJ mol^{-1}), but with regard to indazole **1** itself (27.45 kJ mol^{-1}), the annelation in [*e*] and [*g*] stabilizes further the 1*H*-tautomer whereas the annelation in [*f*] produces the opposite effect. This agrees with the Mills–Nixon rule.[7] The presence of a nitro group at position 3, **51**, further increases the stability of the 2*H*-tautomer **49b** (6.24 kJ mol^{-1}) (an ester group, **52**, produces a similar effect, 4.27 kJ mol^{-1}).

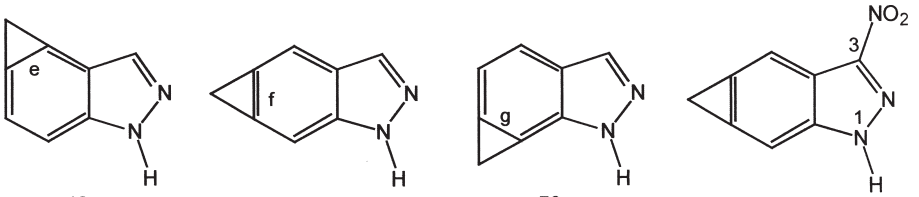

48a **49a** **50a** **51a**

Scheme 4. Methyleneindazoles

Ab initio calculations (B3LYP/6–31G*)

The results obtained at the B3LYP/6–31G* level are reported in Table 4. According to our previous results, the 1*H*-tautomer **1a** was more stable than the 2*H*-tautomer **1b** by $\Delta\Delta E = 15.1\,\mathrm{kJ\,mol^{-1}}$ and $\Delta G^{\circ}_{298.15} = 17.2\,\mathrm{kJ\,mol^{-1}}$ (MP2/6–31G*).[2] The results in Table 4 (B3LYP/6–31G*) are higher, 21.4 and 22.3 $\mathrm{kJ\,mol^{-1}}$, respectively. At a higher level (G2 calculations), the last value change to $\Delta G^{\circ}_{298.15} = 20.3\,\mathrm{kJ\,mol^{-1}}$, intermediate between the MP2/6–31G* and the B3LYP/6–31G* calculated values.

Table 4. Energies (hartree), ΔZPE ($\mathrm{kJ\,mol^{-1}}$), differences in energy (tautomer **b**—tautomer **a**) ($\mathrm{kJ\,mol^{-1}}$) and differences in dipole moments (D)

Compound	Tautomer **a**	Tautomer **b**	$\Delta\Delta E$	$\Delta\Delta E$ + ZPE	$\Delta\Delta G$	$\Delta\mu$
1	−379.84355	−379.83540	21.39	21.98	22.32	0.71
3	−610.90371	−610.89692	17.83	18.78	18.99	0.96
5	−607.72038	−607.72079	−1.06	0.13	0.81	−1.32
7	−584.33970	−584.33591	9.89	10.41	11.18	−3.32
10	−395.87841	−395.87214	16.44	17.41	17.77	−2.05
11	−395.87961	−395.87112	22.30	22.82	23.10	1.61
12	−395.87739	−395.86984	19.79	20.42	20.73	3.72
13	−395.88493	−395.87225	33.30	33.42	33.64	2.81
14	−411.88004	−411.87236	20.17	21.20	21.54	−0.67
15	−411.91482	−411.90894	15.44	16.47	16.80	1.14
16	−411.91494	−411.90454	27.31	27.97	28.22	1.23
17	−411.88154	−411.87485	17.59	18.09	18.27	2.95
18	−411.92332	−411.91071	33.10	33.25	33.44	4.20
19	−411.88390	−411.87049	35.22	35.52	35.75	4.00
20	−427.88824	−427.88224	15.74	16.65	16.87	1.21
21	−427.91894	−427.90731	30.54	31.31	31.57	1.70
22	−427.91621	−427.90497	29.50	30.36	30.62	3.64
23	−427.89372	−427.88198	30.81	31.00	31.11	4.02
24	−443.89503	−443.88443	27.83	28.53	28.64	2.84
25	−533.49119	−533.48643	12.50	12.85	13.05	0.38
26	−533.48244	−533.47039	31.65	32.58	33.19	1.27
27	−533.49065	−533.48707	9.39	10.04	10.36	0.52
28	−687.13759	−687.13564	5.14	5.70	5.94	0.15
29	−763.37303	−763.37107	5.17	5.68	5.96	0.25
30	−687.13247	−687.13062	4.88	5.02	5.12	0.84
35	−549.52690	−549.50973	45.07	45.38	45.73	2.62
39	−565.52824	−565.52511	8.22	9.21	9.52	−1.53
Nitro derivatives						
40	−632.36959	−632.36744	5.66	6.78	9.02	−2.22
41	−770.01294	−770.01364	−1.85	−0.61	2.66	−3.57
42	−967.86345	−967.86684	−8.91	−8.33	−7.51	−3.31
43	−891.62825	−891.63011	−4.86	−4.78	−4.14	−3.77
Ester derivatives						
44	−655.75873	−655.76129	−6.72	−5.01	−3.58	0.74
45	−793.39919	−793.40453	−14.03	−12.12	−10.09	−3.87
46	−991.24276	−991.25107	−21.81	−20.02	−19.09	−1.10
47	−915.00887	−915.01517	−16.52	−15.83	−15.28	−1.89
Methylene derivatives						
48	−417.85038	−417.84256	20.53	21.11	20.86	0.59
49	−417.85460	−417.84803	17.26	17.56	19.99	0.48
50	−417.85116	−417.84228	23.30	23.72	23.83	1.39
51	−622.35116	−622.34891	5.89	6.10	6.95	−3.23
52	−645.73147	−645.73342	−5.11	−4.16	−3.37	−1.35

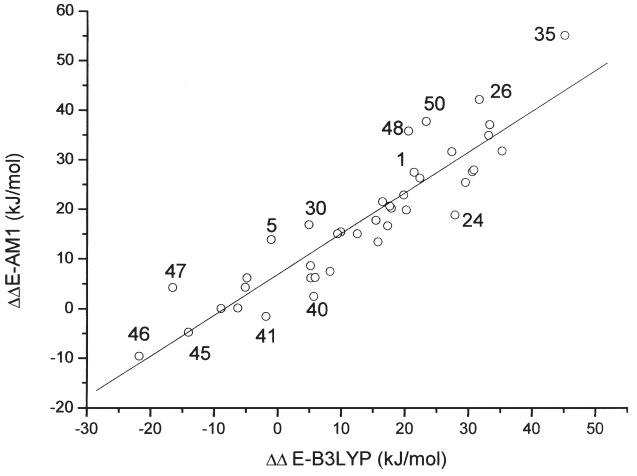

Figure 1. Plot of $\Delta\Delta E$ AM1 vs $\Delta\Delta E$ B3LYP/6–31G* (all values in kJ mol^{-1})

The relationship between AM1 and DFT calculations is reported in Fig. 1.

$$\Delta\Delta E(\text{AM1}) = (6.9 \pm 1.2) + (0.82 \pm 0.06)\,\Delta\Delta E(\text{B3LYP}),\ n = 40,\ r^2 = 0.836$$

The largest deviations (>10 kJ mol^{-1}) are found for **24** (−11.0), **35** (+11.1), **47** (+10.9), **48** (+12.0) and **50** (+11.7 kJ mol^{-1}). Assuming that the DFT calculations are closer to the experimental reality, the AM1 calculations overestimate ΔE in most cases (3-CO_2Me, benzo[*f*], benzo[*f*]-7-aza, methylene[*e*] and methylene[*g*]) and underestimate ΔE in the case of the 4,5,6,7-tetraaza derivative **24**. In this last case, it is the lone pair–lone pair (LP–LP) repulsion of the four adjacent pyridine-like nitrogen atoms that is underestimated by the semi-empirical method.

Using a Free–Wilson model (presence–absence matrix),[20] the 40 data in Table 4 can be analyzed to find individual contributions. A preliminary multi-regression shows that the contribution of N-5 is not significant and was withdrawn and the multi-regression repeated (Table 5, $n = 40$, $r^2 = 0.990$, *F*-value 173.7, *P*-value <0.0001) (others are almost not significant: 3-C_6H_5, 6-N and methylene[*e*]).

Pyrazolo[3,4-*b*]quinoline (+45.07) is the indazole having the most stable 1*H*-tautomer (**35a**), whereas that with the most stable 2*H*-tautomer is the methyl ester of the phenanthroindazole-3-carboxylic acid (**46**) (−21.81 kJ mol^{-1}). Concerning compounds without 3-NO_2 or 3-CO_2Me substituents, the indazole with the most stable 2*H*-tautomer is dibenzo[*e*,*g*]indazole (+5.14 kJ mol^{-1}) (**28**).

Only two 3-substituents produce large effects, the nitro and the ester. We carried out a Bader AIM analysis[22] of 2*H*-3-CO_2CH_3-indazole (**5b**) and 2*H*-3-NO_2-indazole (**7b**), showing that in no case is there a bcp (bond critical point) corresponding to an N—H···O hydrogen bond (note that the N—H···O angle is 90–91°, not favorable to an intramolecular hydrogen bond. In the case of NH-pyrazoles, the 5-position is preferred by the ester group, which corresponds to a 2*H*-indazole,[23] probably because there is a LP–LP repulsion between the oxygen atoms of the ester group and the N-2 atom of pyrazole or indazole in tautomer **a**.

In Scheme 5 we show some structural effects from Table 5. Since they correspond to energy differences, the origin of the effect can be found on **a**, on **b** or on both. The 7-aza effect is probably due to a destabilization of the 2*H*-tautomer by LP–LP repulsion between the N atoms at positions 2 and 7. The benzo effects are important and the sign depends on the [*e*], [*f*] or [*g*] position. They are due to a localization of the π-system in the benzene ring of indazole. The Mills–Nixon effect (not depicted in Scheme 5) is observed for methylene compounds but much attenuated compared with those described for pyrazoles.[21]

The difference in dipole moments reported in Table 4 allows one to predict qualitatively the effect of polar solvents, e.g. water (note that compounds even sparingly soluble in water are suitable for tautomeric studies using electronic spectra). If $\Delta\mu > 0$, a polar solvent should favor tautomer 2*H*(**b**), this being the case for most compounds. If $\Delta\mu < 0$, a polar solvent should favor tautomer 1*H*(**a**), this being the case for the nitro derivatives and, to a minor extent, the ester derivatives. Therefore, the solvent polarity opposes the tendency found in the gas phase.

Table 5. Individual contributions in kJ mol^{-1}[a]

Substituent	Value	Substituent	Value	Substituent	Value
3-C_6H_5	−2.4 ± 2.1	Benzo[*e*]	−4.6 ± 1.3	Methylene[*e*]	−1.5 ± 1.5
3-CO_2CH_3	−22.8 ± 1.0	Benzo[*f*]	11.6 ± 1.6	Methylene[*f*]	−2.9 ± 2.1
3-NO_2	−11.0 ± 1.0	Benzo[*g*]	−9.6 ± 1.1	Methylene[*g*]	3.1 ± 2.1
4-N	−2.7 ± 0.8	Phenanthro	−17.4 ± 1.4		
6-N	−1.0 ± 0.9	Naphtho[*g*]	−14.4 ± 1.4		
7-N	13.2 ± 0.9				

[a] Intercept 20.2 ± 0.08.

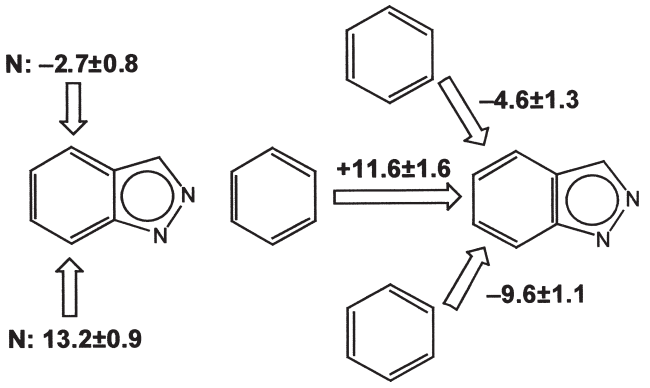

Scheme 5. Aza and benzo structural effects on the **a**/**b** tautomerism of indazoles (values in kJ mol^{-1}) based on B3LYP calculations and Free–Wilson model. These values are contributions with regard to **1** ($\Delta\Delta G = +22.3$ kJ mol^{-1})

CONCLUSIONS

The experimental results (concerning the tautomerism of **2a**, **3a**, **5a**, **8a**, **9a**, **18a**, **28a**, see the Introduction) are well reproduced by the calculations.

The additive model works well, mainly with the DFT values ($r^2 = 0.99$).

In studies concerning tautomerism, the inexpensive AM1 method can be used as an exploratory tool.

We have found several candidates for indazoles where the theory (AM1/B3LYP) predicts the 2*H*-tautomer (**b**) to be more stable than the 1*H*-tautomer (**a**).

The main structural factors that stabilize the 2*H*-tautomer are the 3-methoxycarbonyl and 3-nitro substituents and the benzo[*e*], benzo[*g*], naphtho[*g*] and phenanthro annelations.

Acknowledgments

Financial support was provided by the Spanish DGICYT (Projects SAF2003-08003-C02-02 and BQU-2000-0906).

REFERENCES

1. Minkin VI, Garnovskii DG, Elguero J, Katritzky AR, Denisko OV. *Adv. Heterocycl. Chem*. 2000; **76**: 157–323 (see 175–176).
2. Catalán J, de Paz JLG, Elguero J. *J. Chem. Soc., Perkin Trans. 2* 1996; 57–60.
3. Ögretir C, Kaypak NF. *THEOCHEM* 2002; **583**: 137–144; Ögretir C, (Kaypak) Tay NF. *THEOCHEM* 2002; **583**: 145–153.
4. Borges F, Fernandes E, Roleira F. *Curr. Med. Chem*. 2002; **9**: 195–217.
5. Elnagdy MH, Elmoghayar MRH. *Adv. Heterocycl. Chem*. 1987; **41**: 319–376.
6. Korpi ER, Uusi-Oukari M, Wegelius K. *Eur. J. Pharmacol*. 1992; **213**: 323–329.
7. Catalán J, Claramunt RM, Elguero J, Laynez J, Menéndez M, Anvia F, Quian JH, Taagepera M, Taft RW. *J. Am. Chem. Soc*. 1998; **110**: 4105–4111.
8. García MA, López C, Claramunt RM, Kenz A, Pierrot M, Elguero J. *Helv. Chim. Acta* 2002; **85**: 2763–2776.
9. Glaser R, Mummert CL, Horan CJ, Barnes CL. *J. Phys. Org. Chem*. 1993; **6**: 201–214.
10. Ballesteros P, Elguero J, Claramunt RM, Faure R, Foces-Foces C, Hernández-Cano F, Rousseau A. *J. Chem. Soc., Perkin Trans. 2* 1986; 1677–1681; Schilf W, Stefaniak L, Witanowski M, Webb GA, Braun S. *Pol. J. Chem*. 1986; **60**: 151–155; Schilf W, Stefaniak L, Webb GA. *Magn. Reson. Chem*. 1987; **25**: 721–724.
11. Faure R, Llinares J, Elguero J, Goya P. *Bull. Soc. Chim. Belg*. 1987; **96**: 603–617; Claramunt RM, Sanz D, López C, Jiménez JA, Jimeno ML, Elguero J, Fruchier A. *Magn. Reson. Chem*. 1997; **35**: 35–76.
12. López C, Claramunt R, Trofimenko S, Elguero J. *Can. J. Chem*. 1993; **71**: 679–684.
13. *Chem3D Pro, Version 4.0*. CambridgeSoft: Cambridge, 1997.
14. Frisch MJ, Trucks GW, Schlegel HB, Scuseria GE, Robb MA, Cheeseman JR, Zakrzewski VG, Montgomery JA, Stratmann RE, Burant JC, Dapprich S, Millam JM, Daniels AD, Kudin KN, Strain MC, Farkas O, Tomasi J, Barone V, Cossi M, Cammi R, Mennucci B, Pomelli C, Adamo C, Clifford S, Ochterski J, Petersson GA, Ayala PY, Cui Q, Morokuma K, Malick DK, Rabuck AD, Raghavachari K, Foresman JB, Cioslowski J, Ortiz JV, Stefanov BB, Liu G, Liashenko A, Piskorz P, Komaromi I, Gomperts R, Martin RL, Fox DJ, Keith T, Al-Laham MA, Peng CY, Nanayakkara A, Gonzalez C, Challacombe M, Gill PMW, Johnson BG, Chen W, Wong MW, Andres JL, Head-Gordon M, Replogle ES, Pople JA. *Gaussian 98*. Gaussian: Pittsburgh, PA, 1998.
15. Becke AD. *J. Chem. Phys.* 1993; **98**: 5648–5652; Lee C, Yang W, Parr RG. *Phys. Rev. B* 1988; **37**: 785–789.
16. Hariharan PA, Pople JA. *Theor. Chim. Acta* 1973; **28**: 213–222.
17. Pople JA, Krishnan R, Schlegel HB, Binkley JS. *Int. J. Quantum Chem. Symp*. 1979; **13**: 225–241; Saxe P, Yamaguchi Y, Schaefer HF. *J. Chem. Phys*. 1982; **77**: 5647–5654.
18. Frisch MJ, Pople JA, Krishnam R, Binkley JS. *J. Chem. Phys.* 1984; **80**: 3265–3269.
19. Curtiss LA, Raghavachari K, Trucks GW, Pople JA. *J. Chem. Phys*. 1991; **94**: 7221–7230; Curtiss LA, Raghavachari K, Trucks GW, Pople JA. *J. Chem. Phys*. 1993; **98**: 1293–1298; Curtiss LA, Redfern PC, Smith BJ, Radom L. *J. Chem. Phys*. 1996; **104**: 5148–5152.
20. Hansch C, Leo A. *Exploring QSAR: Fundamentals and Applications in Chemistry and Biology*. American Chemical Society: Washington, DC, 1995 (see http://www.chem.swin.edu.au/modules/mod4/qsarwebp6. html); Cativiela C, Elguero J, Mathieu D, Meléndez E, Phan Tan Luu R. *Eur. J. Med. Chem*. 1983; **18**: 359–363; Cativiela C, García JI, Elguero J. *An. Quím*. 1987; **83C**: 278–282; Cativiela C, Elguero J, García JI, Mathieu D. *QSAR Drug Des. Toxicol*. 1987; 55–57; Cativiela C, García JI, Elguero J, Mathieu D, Phan Tan Luu R. *Quant. Struct.*–Act. Relat. 1987; **6**: 173–178; Alkorta I, Elguero J, Rozas I, Balaban AT. *THEOCHEM* 1991; **228**: 47–60.
21. Martínez A, Jimeno ML, Elguero J, Fruchier A. *New J. Chem*. 1994; **18**: 269–277; Ramos M, Alkorta I, Elguero J. *Tetrahedron* 1997; **53**: 1403–1410; Alkorta I, Elguero J. *Struct. Chem*. 1997; **8**: 189–195.
22. Bader RFW. *Atoms in Molecules: A Quantum Theory*. Oxford University Press: New York, 1990.
23. Cabildo P, Claramunt RM, Elguero J. *Org. Magn. Reson*. 1984; **22**: 603–607.